Hindawi
Mathematical Problems in Engineering
Volume 2023, Article ID 1600610, 7 pages
https://doi.org/10.1155/2023/1600610

Research Article

Collective Dynamical Behaviors of Nonlocally Coupled Brockett Oscillators

Janarthan Ramadoss,[1] Premraj Durairaj,[2] Karthikeyan Rajagopal ,[2] and Akif Akgul [3]

[1]*Centre for Artificial Intelligence, Chennai Institute of Technology, Chennai 600069, Tamil Nadu, India*
[2]*Centre for Computation Biology, Chennai Institute of Technology, Chennai 600069, Tamil Nadu, India*
[3]*Department of Computer Engineering, Faculty of Engineering, Hitit University, Corum 19030, Turkey*

Correspondence should be addressed to Akif Akgul; akifakgul@hitit.edu.tr

Received 18 July 2022; Revised 21 October 2022; Accepted 25 November 2022; Published 17 April 2023

Academic Editor: Ji Wang

In this study, we consider a network of nonlocally coupled Brockett oscillators (BOs) with attractive and repulsive (AR) couplings to illustrate the existence of diverse collective dynamical behaviors, whereas previous studies solely concentrated on synchronization. In the absence of coupling, the individual BO oscillator shows stable periodic oscillations (POs) or stable steady state (SS) depending on the critical values of the parameters. We first begin by examining the collective dynamics by setting the critical value of the parameters at the active (PO) region. A diverge collective dynamical states are manifested for a fixed nonlocal coupling range with rising coupling magnitude. Notably, the lower coupling strength exhibits two distinct dynamical patterns at lower and higher transients. At lesser transients, for example, transient dynamics of desynchronization, chimera, and traveling wave states are observed. At larger time periods, the transient dynamics disappear with the emergence of a synchronized state. Increasing the coupling strength results in a unique state of traveling wave or synchronized state for smaller and larger time periods depending on the coupling strength. Increasing the coupling strength further gives rise to clustering behaviors. Importantly, the considered system attains cluster oscillation death (COD) through a cluster oscillatory state (COS). Finally, there exists a chimera death at a larger coupling strength. The observed dynamical transitions are further demonstrated through the two-parameter analysis by setting different critical thresholds.

1. Introduction

Complex systems around us, such as social systems, biological networks, and power grids, comprise a large number of individual constituents, and they interact to yield a wide range of macroscopic cooperative states. Understanding such a complicated system can be aided by mathematical modeling. Depending on the needs of system behavior, distinct chaotic and periodic oscillator models have been established [1–5]. To mimic the behavior of the complex system, the number of individual constituents connected under various coupling interactions, including local, global, and nonlocal coupling connectivities, as well as more complex interactions like random, small-world, and scale-free connectivities. Such a framework of network can act as an excellent platform for replicating the dynamical behavior of many natural and man-made complex systems. Importantly, coupling interaction among elements plays a crucial role. Moreover, depending on the involved parameters, coupling architecture, and static and dynamic interaction among the coupled elements, the system shows various kinds of synchronization [6], traveling waves [7, 8], chimera [9, 10], cluster [11, 12], oscillation quenching states [13–15], and so on. In particular, heterogeneously and nonlinearly coupled phase oscillators, AR coupled Stuart–Landau oscillators, coupled Lorenz oscillators, and other systems have reported the existence of various collective dynamical behaviors [16–18]. Each of these has a strong resemblance with many real-life instances.

Among the collective dynamical states previously mentioned, oscillation quenching is an intriguing phenomenon having implications in many practical situations where undesired fluctuations need to be suppressed [19, 20]. To better comprehend the situations in which the system can experience oscillation quenching, various analyses have been conducted. The results have shown that coupled systems with a small number of oscillators can achieve oscillation quenching or steady states under distinct conditions or interactions among the nodes, such as parameter mismatch, time-delay coupling, conjugate coupling, and mixed attractive and repulsive couplings [6, 21–23]. In addition, depending on the steady state, the oscillation quenching state can be categorized as either a homogeneous steady state (trivial amplitude death and nontrivial amplitude death states) or an inhomogeneous steady state (oscillation death state) [19, 20]. Following that, different types of oscillation quenching states, such as cluster oscillation death, chimera death, and incoherent oscillation death states, have been revealed in a network of coupled systems as a result of system characteristics, connection architecture, and network interaction strength [24–26].

However, the presence of multiple interactions in a realistic system, it is interesting to investigate the presence of multiple couplings in the same system at the same time. As a result, mixed attractive and repulsive (AR) couplings have been considered an account. Such mixed attractive and repulsive (AR) couplings are more realistic than other interactions, and they can help to unravel a variety of realistic phenomena. Moreover, such couplings can also be viewed as positive-negative feedback in biological systems, excitatory-inhibitory coupling in neural networks, and contrarian-conformist in social networks. Hence, it is intriguing to figure out how AR coupling exhibits collective dynamics. As a consequence, using the various periodic, chaotic, and neural systems, the competing effects of AR couplings have been demonstrated. For instance, the existence of different synchronization, spontaneous symmetry breaking states, and oscillation death states has been identified due to the trade-off between AR couplings in the minimal network of two or three coupled limit-cycle oscillators [6, 27, 28]. Later, the studies were extended to the network of coupled oscillators with AR coupling. Substantially, the emergence of several dynamical behaviors such as chimera, solitary state, traveling wave state, and different oscillation quenching states including chimera death and cluster death states was discovered [9, 24]. In addition, the interplay between the AR couplings is also analyzed in the network of chaotic as well as neuronal systems [29, 30]. Through the Lorentz system, it was demonstrated the coexistence of amplitude death with complete synchronization or antiphase synchronization [31]. Also, the occurrence of explosive transitions was recently proved by utilizing these mixed couplings [32, 33]. Furthermore, such coupling strategies were implemented as nonlinear couplings or extended to multilayer networks [34, 35].

On the other hand, the Brockett oscillator is a well-known periodic oscillator that has received little attention in the literature [36]. Initially, BO was used to analyze robust synchronization [37]. Later, the nonidentical BO-induced global synchronization was reported [38]. It is further proved that the observed global synchronization has applications in power-grid synchronization and renewable energy sources [39]. Further, the global synchronization was also verified experimentally in a network of Brockett oscillators using analog circuit realizations [40]. According to the reports, Brockett oscillator has only been investigated from the standpoint of synchronicity up to these days. Besides that, the above discussion shows that the attractive and repulsive can exhibit diverse collective behaviors as a result of the competitive interaction among couplings. As a consequence, we investigate whether nonlocally coupled Brockett oscillators can exhibit collective dynamics other than synchronization when coupled with attractive and repulsive couplings. The majority of previous research has focused solely on the phenomenon of synchronization. Thus, we construct a network of nonlocally coupled oscillators with a mix of attractive and repulsive couplings. In particular, we address the potential collective dynamics detected by the model under consideration in this study, such as transient chimera, traveling waves, cluster oscillatory states, and distinct oscillation death states, respectively. Specifically, we delineate the dynamical behaviors at the lower and higher transients.

The remaining sections of the article are structured as follows. Section 2 introduces the nonlocally coupled Brockett oscillators. The dynamical transitions are then described in Section 3 as varying the coupling strength by using spatiotemporal patterns and two-parameter analysis. Finally, in Section 4, the conclusion will be presented.

2. The Model

To illustrate the collective dynamical states, we consider a general mathematical model of a Brockett oscillator (BO). Originally, the Brockett oscillator was introduced by R. Brockett in 2013, to study the global synchronization [36–38]. Following that, the majority of earlier work on BO focused completely on synchronization behaviors. The dynamical equation for BO can be expressed as

$$\ddot{x} + \alpha\dot{x}\left(\dot{x}^2 + x^2 - 1\right) + x = \alpha^2 u, \tag{1}$$

where x is the state variable representing the amplitude of the system; α is the constant parameter fixed as $\alpha = 1.0$ throughout the study; and u is the critical control parameter for the active state, $|u| \leq \dot{x}^2 + x^2$. To obtain the active (oscillatory) region, the one-parameter bifurcation diagram is plotted using equation (1) by varying the controlling parameter "u" in Figure 1. It is observed that there is a transition from stable periodic oscillation (active) to stable steady state (inactive) through Hopf bifurcation. The stable periodic oscillation (denoted by green-filled circles connected by a line) exists when $0 \leq |u| \leq 1$. Also, the amplitude of periodic oscillations decreases when it becomes zero at which Hopf bifurcation occurs.

In addition, to inspect whether a network BO can also exhibit other collective dynamical behaviors, we consider the

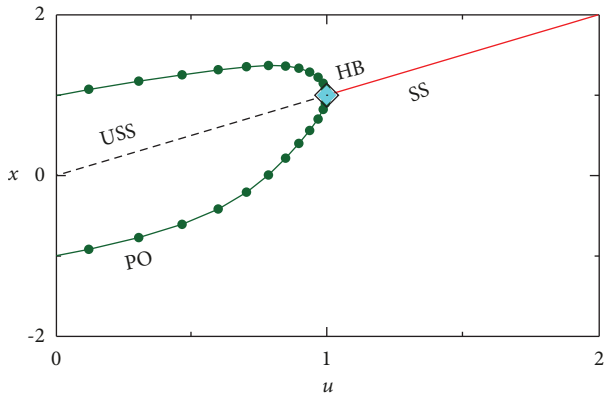

Figure 1: One-parameter bifurcation diagram (created with the XPPAUT program) for $\alpha = 1.0$ illustrates the transition from stable periodic oscillation to a stable steady state via Hopf bifurcation by varying the parameter u. HB is the Hopf bifurcation designated by diamond point. The line connected by filled circles represents the periodic oscillation (PO). The solid (red) and dashed (black) lines denote the stable steady (SS) state and unstable steady state (USS), respectively.

ring network of nonlocally coupled BOs with attractive and repulsive couplings which can be written as

$$\dot{x}_i = y_i + \frac{\varepsilon}{2P}\sum_{j=i-p}^{i+p}\left(x_j - x_i\right), i = 1, 2, \ldots, M,$$

$$\dot{y}_i = \alpha^2 u - \alpha\left(x_i^2 + y_i^2 - 1\right)y_i - x_i - \frac{\varepsilon}{2P}\sum_{j=i-p}^{i+p}\left(y_j - y_i\right), \tag{2}$$

where x_j and y_j are the state variables of BOs. M is the chosen number of oscillators ($M = 100$) in the network and ε is the coupling strength. P is the total number of nearest neighbors in both directions of the ring and the nonlocal coupling radius (R) is given by $R = P/M$. The numerical simulations are carried out using the RK_4 algorithm with fixed step size $h = 0.01$ and random initial states. The dynamical characteristics of system (2) are investigated in the following sections by fixing the magnitude of u in the active region $(0 \le u \le 1)$.

3. Dynamical Transitions for Different Critical Thresholds

Many real-world instances can be seen by exploring collective patterns in coupled oscillations. The clear observation of such patterns can be useful for controlling them or identifying the circumstances in which they may exist.

To manifest the existence of distinct collective dynamical state, the spatiotemporal patterns and snapshots are plotted in Figure 2 by fixing the control parameter at active region $u = 0.0$, and other parameter values are fixed as $\alpha = 1.0, R = 0.2$, and $M = 100$. Specifically, the spatiotemporal patterns are depicted for the dynamical behaviors at the lower and the higher values of the time period, to understand the long-lasting dynamical behaviors. As a result, the dynamics at a lower time period $(2000 \le t \le 2030)$ are shown in the lower portion of the spatiotemporal pattern. The dynamical behavior is then depicted in the upper portion of the spatiotemporal pattern after a long transient for the period $(200000 \le t \le 200030)$. If the coupling strength is very low at $\varepsilon = 0.01$, the lower transients show the desynchronization (DS) behavior as shown in Figure 2(a). The oscillators in the DS state are randomly distributed as shown in Figure 2(e). Further, after a long transient, the system attains the synchronization (SYN) behavior (see the upper portion of the spatiotemporal plot). By slightly increasing the coupling strength, $\varepsilon = 0.05$, some of the oscillators in the desynchronized state exhibit coherent behaviors while the others exhibit incoherent behavior (see Figures 2(b) and 2(f)). Such a coexistence of coherent and incoherent behaviors is referred to as chimera behavior. After a long transient, the remaining desynchronized oscillators also reach the coherent behaviors and the system shows the synchronization behavior. Since loses the chimera behavior at large transient it is called a transient chimera (TC) state. Further, increasing the coupling strength to $\varepsilon = 0.2$, at the lower values time period result in transient traveling wave (TTW), while increasing the time period gives rise to synchronization behavior (see Figures 1(c) and 2(g).

Upon increasing the coupling strength to $\varepsilon = 0.55$ and $\varepsilon = 0.65$, the system shows a traveling-wave state and a synchronized state for lower and higher time periods as portrayed in Figures 2(d), 2(h), 2(i), and 2(m). On increasing the coupling strength further to $\varepsilon = 0.75$, we observed the cluster oscillatory (COS) state where the existence of inhomogeneous oscillators oscillates either upper and the lower branch while the homogeneous oscillators at the edges of inhomogeneous oscillators as in Figures 2(j) and 2(n). When the coupling strength is increased still more to $\varepsilon = 0.85$, the oscillators in the homogeneous state also attain the inhomogeneous state and exhibit the cluster oscillation death (COD) state. The number of patches in the cluster oscillation death at lower and higher time periods is the same, as illustrated in Figures 2(k) and 2(o). Furthermore, with higher coupling, we found chimera death (CD), which is the coexistence of coherent and incoherent oscillation death states, as illustrated in Figures 2(l) and 2(p) for lower and higher time periods. From the observation, we identified that the transient dynamics are observed only at lower values of coupling strength. Also, it is observed that the structure of observed oscillation death states is similar for lower and higher values of time period.

Additionally, the occurrence of incoherent oscillation death (IOD) state is noticed at $P = 1$ where the oscillators have interacted with a local nearest neighbor, that is, the oscillators are connected only with the closest nearest neighbor in both directions of the ring. In the IOD state, all the oscillators attain the upper and lower branches of the inhomogeneous state alternatively, which is clear from the spatiotemporal pattern and snapshot in Figures 3(a) and 3(b). For the purpose of determining the fixed point solution for the IOD state, it is assumed that an odd number of

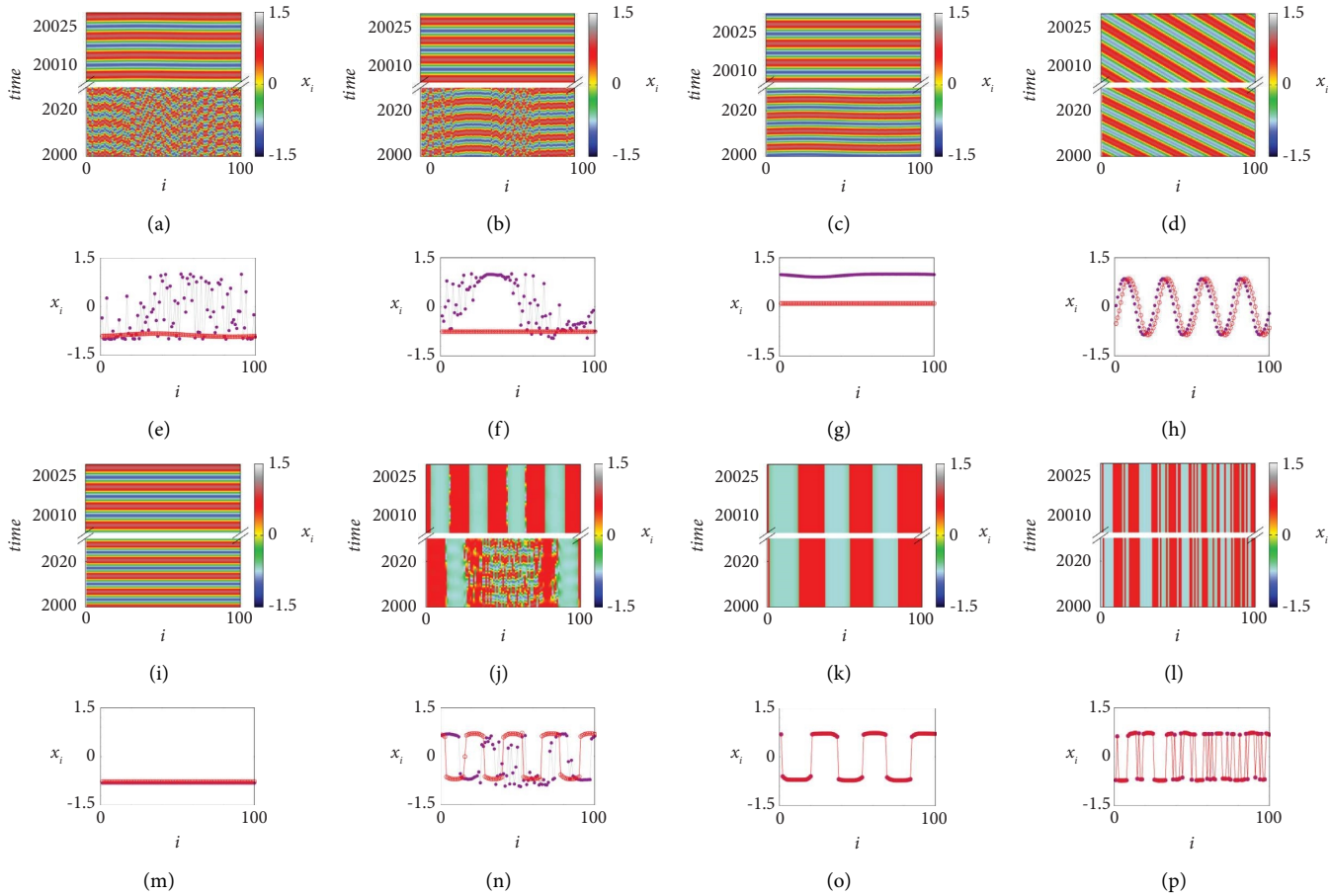

FIGURE 2: Space-time diagram and snapshot of nonlocally coupled Brockett oscillators with attractive and repulsive couplings for (a) transient desynchronized state ($\varepsilon = 0.01$), (b) transient chimera ($\varepsilon = 0.05$), (c) transient traveling wave ($\varepsilon = 0.2$), (d) traveling wave ($\varepsilon = 0.55$), (i) synchronized state ($\varepsilon = 0.65$), (j) cluster oscillatory state ($\varepsilon = 0.75$), (k) cluster oscillation death ($\varepsilon = 0.85$), and (l) chimera death ($\varepsilon = 1.0$). In the space-time diagram, the lower portion is obtained after transient 2×10^3 time units, and the upper portion is observed after transient 2×10^4 time units. The second panel (e–h) and fourth panel (m–p) are the corresponding snapshots of first panel (a–d) and third panel (i–l), respectively. Lower transients display the dynamical transition from desynchronized state to chimera death through transient chimera, transient traveling waves, synchronization, cluster oscillatory states, and cluster oscillation death states for the given coupling strength, whereas larger transients exhibit the transition from synchronized state to chimera death through the traveling wave state and cluster oscillation death states. Other parameters are fixed as $R = 0.2$, $\alpha = 1.0$, $u = 0.0$, and $M = 100$.

oscillators takes the value $(x_i, y_i) = (x_0, y_0)$ and an even number of oscillators takes the value $(x_i, y_i) = (-x_0, -y_0)$. By substituting this in equation (2) and taking into account $(\dot{x}, \dot{y}) = (0, 0)$, the simplified form of equation can take the form

$$\begin{aligned} \dot{x}_0 &= y_0 - \beta x_0, \\ \dot{y}_0 &= \alpha^2 u - \alpha\left(x_0^2 + y_0^2 - 1\right) y_0 - x_0 + \beta y_0, \end{aligned} \tag{3}$$

where $\beta = 2P\varepsilon$ for odd nearest neighbour P and $\beta = (2P + 1)\varepsilon$ for even range of P. By solving equation (3), we can get the solution for IOD state as given below.

$$\begin{aligned} x_0 &= \mp \frac{2 * 3^{1/3}\alpha\beta\left(\beta^4 + \alpha\left(\beta + \beta^3\right) - 1\right) + 2^{1/3}\tilde{\eta}^{1/3}}{6^{2/3}\alpha\beta\left(1 + \beta^2\right)\tilde{\eta}^{1/3}}, \\ y_0 &= \beta x_0, \end{aligned} \tag{4}$$

where $\tilde{\eta} = -9u\alpha^4(\beta + \beta^3)^2 + 1/3\sqrt{729u^2\alpha^8(\beta + \beta^3)^4 - 108(\beta^2 + \alpha\beta - 1)^3(\alpha\beta + \alpha\beta^3)^3}$. It is verified that the IOD state solution from equation (4) exactly matches with the numerically obtained solution.

Analyzing the dynamical transitions in parametric space under various values of parameter u can facilitate determining the impact of such parameter in exhibiting various collective dynamical and its spread across the parameter space. Thus, to illustrate the global dynamical transitions, the two-parameter diagram is portrayed in (ε, R) parametric space in Figure 4 by fixing the three different critical values of u. The region for each dynamical state is obtained after removing the transient 2×10^3 time units. Figure 4(a) is depicted for $u = 0.0$, and it is observed that for all values of the nonlocal coupling range, there exists a transition from transient desynchronization to transient traveling wave through transient chimera as a function of coupling strength. By increasing the magnitude coupling strength, it is

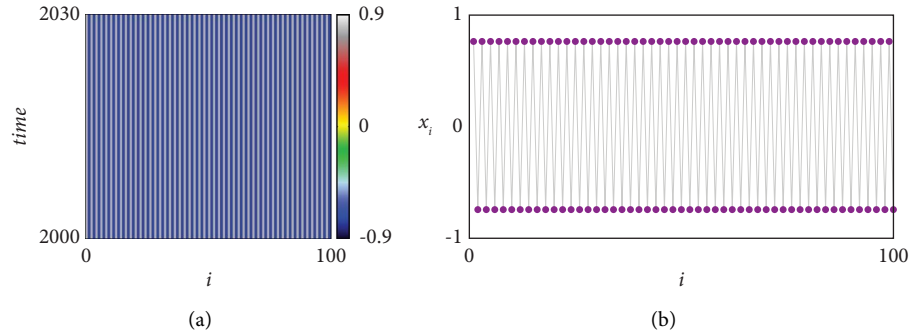

Figure 3: (a) Space-time diagram and (b) snapshot of an incoherent oscillation death (IOD) state in which the oscillators alternately shift between the upper and lower branches of inhomogeneous stable states for $R = 0.01$ $(P = 1)$. Other parameters are fixed as $\alpha = 1.0$, $M = 100$, $u = 0.0$, and $\varepsilon = 0.85$, respectively.

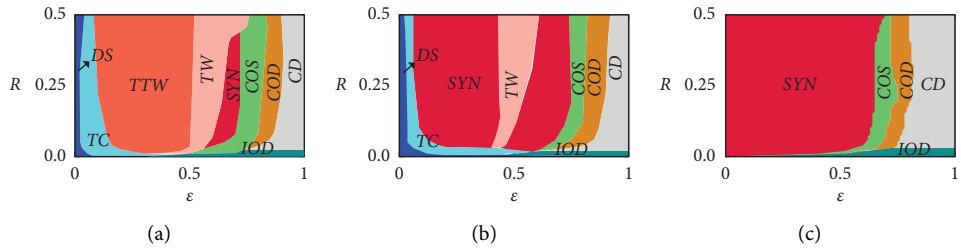

Figure 4: Two-parameter diagram in (ε, R) space (after transient 2×10^3 time units) for (a) $u = 0.0$, (b) $u = 0.5$, and (c) $u = 1.0$. DS, TC, and TTW are the transient oscillatory states of transient desynchronized state, transient chimera, and transient traveling wave state, respectively. TW, SYN, and COS are traveling wave, synchronization, and cluster oscillatory states, respectively. COD and CD are the oscillation death states, namely, cluster oscillation death and chimera death, respectively. It is evident that decreasing the synchronization region with respect to the parameter u while increasing collective dynamical states in the parametric space (ε, R).

noticed that transition to traveling wave and synchronization. Also, one can note that the raising coupling strength further gives rise to cluster behavior. Particularly, the transition to cluster oscillation death state takes place through the cluster oscillatory state. Finally, there exists a chimera death region at large coupling strength. Importantly, it can also be noted that the sufficient strength of coupling strength with minimal nearest neighbors $(P \leq 2)$ shows the incoherent oscillation death state. Analogously, Figures 4(b) and 4(c) are plotted for $u = 0.5$ and $u = 1.0$. Increasing the critical value $u = 0.5$ suppresses the transient traveling wave with the stabilization of the synchronized state. As a result, the synchronization region is getting increased. Interestingly, we observed a swing of synchronization behavior in Figure 4(b), that is, the SYN state is destabilized with the emergence of TW, and it is again restabilized with the suppression of TW as a function of ε. Upon increasing the critical value to $u = 1.0$, as shown in Figure 4(c), we identified the TW, DS, and TC regions which are also suppressed with the stabilization of the synchronized state. As a result, we obtained a wide synchronization region.

According to the findings, increasing the control parameter u broadens the synchronization state region while suppressing many other collective dynamical states.

4. Conclusions

Understanding the macroscopic collective states is still an open topic of research, and there is an increasing research interest among scientists. In this study, we used nonlocally coupled Brockett oscillators with mixed attractive and repulsive couplings to demonstrate the occurrence of distinct collective dynamical states. To do so, we first demonstrated the behavior of a single BO using a one-parameter bifurcation diagram, and it is discovered that there is a shift from periodic oscillation to a stable steady state via Hopf bifurcation. We then extended this to the network of coupled systems that exhibit the transition from different dynamical states as a function of coupling strength. Most importantly, we discovered the occurrence of a few transient dynamics at shorter time periods as compared to dynamics at larger time periods. For example, when the coupling strength is low, we observed a desynchronized state, chimera, and traveling wave as transient states detected at lower time periods. When we increase the time periods while keeping the coupling strength the same, the transient dynamics approach the synchronization state. When the coupling strength was raised, the behavior for lower and higher time periods was unchanged. We found a significant transition from synchronization to chimera via the traveling wave,

cluster oscillatory state, and cluster oscillation death state. Finally, we proved dynamical transitions in parametric spaces by assigning different values to the critical threshold. We found that raising the threshold reduces the region of transient dynamics by widening the synchronization state region. In addition, we deduced the analytical solution for incoherent oscillation death state. We believe that obtained results will offer new insight and aid in the discovery of the collective dynamical behavior of periodic oscillators with biological applications including neural networks as well as power networks.

Furthermore, the study may raise a number of unresolved scientific and engineering issues. Many complex real-world networks, for example, have intricate connectivities and a larger number of constituents. As a result, it will be required to widen the analysis to include random, small-world, and scale-free interactions; this will aid in understanding the necessary conditions for collective dynamical behavior to emerge. Furthermore, many practical systems typically involve noise. As a result, it will be interesting to investigate the impact of noise in coupled BOs. This analysis can also be extended to fractional-order systems, which are more relevant to realistic real-world systems.

Data Availability

The data used to support the findings of this study are included within the article.

Conflicts of Interest

The authors declare that they have no conflicts of interest.

Acknowledgments

This study was funded by the Center for Nonlinear Systems, Chennai Institute of Technology (CIT), India, with funding number: CIT/CNS/2022/RP-016. The authors are grateful for the support.

References

[1] F. Nazarimehr, K. Rajagopal, J. Kengne, S. Jafari, and V. T. Pham, "A new four-dimensional system containing chaotic or hyper-chaotic attractors with no equilibrium, a line of equilibria and unstable equilibria," *Chaos, Solitons & Fractals*, vol. 111, pp. 108–118, 2018.

[2] K. Rajagopal, A. Bayani, A. J. M. Khalaf, H. Namazi, S. Jafari, and V. T. Pham, "A no-equilibrium memristive system with four-wing hyperchaotic attractor," *AEU-International Journal of Electronics and Communications*, vol. 95, pp. 207–215, 2018.

[3] K. Rajagopal, A. Akgul, S. Jafari, and B. Aricioglu, "A chaotic memcapacitor oscillator with two unstable equilibriums and its fractional form with engineering applications," *Nonlinear Dynamics*, vol. 91, no. 2, pp. 957–974, 2018.

[4] K. Rajagopal, S. Jafari, A. Karthikeyan, A. Srinivasan, and B. Ayele, "Hyperchaotic memcapacitor oscillator with infinite equilibria and coexisting attractors," *Circuits, Systems, and Signal Processing*, vol. 37, no. 9, pp. 3702–3724, 2018.

[5] D. Premraj, K. Manoj, S. A. Pawar, and R. I. Sujith, "Effect of amplitude and frequency of limit cycle oscillators on their coupled and forced dynamics," *Nonlinear Dynamics*, vol. 103, no. 2, pp. 1439–1452, 2021.

[6] K. Sathiyadevi, S. Karthiga, V. K. Chandrasekar, D. V. Senthilkumar, and M. Lakshmanan, "Spontaneous symmetry breaking due to the trade-off between attractive and repulsive couplings," *Physical Review A*, vol. 95, no. 4, Article ID 042301, 2017.

[7] J. Palanivel, K. Suresh, D. Premraj, and K. Thamilmaran, "Effect of fractional-order, time-delay and noisy parameter on slow-passage phenomenon in a nonlinear oscillator," *Chaos, Solitons & Fractals*, vol. 106, pp. 35–43, 2018.

[8] D. Premraj, K. Suresh, T. Banerjee, and K. Thamilmaran, "Control of bifurcation-delay of slow passage effect by delayed self-feedback," *Chaos: An Interdisciplinary Journal of Nonlinear Science*, vol. 27, no. 1, Article ID 013104, 2017.

[9] K. Sathiyadevi, V. K. Chandrasekar, D. V. Senthilkumar, and M. Lakshmanan, "Imperfect amplitude mediated chimera states in a nonlocally coupled network," *Frontiers in Applied Mathematics and Statistics*, vol. 4, p. 58, 2018.

[10] K. Sathiyadevi, V. K. Chandrasekar, and M. Lakshmanan, "Emerging chimera states under nonidentical counter-rotating oscillators," *Physical Review A*, vol. 105, no. 3, Article ID 034211, 2022.

[11] N. Zhao, Z. Sun, and W. Xu, "Enhancing coherence via tuning coupling range in nonlocally coupled Stuart–Landau oscillators," *Scientific Reports*, vol. 8, no. 1, pp. 8721–8812, 2018.

[12] X. Li, T. Qiu, S. Boccaletti, I. Sendiña-Nadal, Z. Liu, and S. Guan, "Synchronization clusters emerge as the result of a global coupling among classical phase oscillators," *New Journal of Physics*, vol. 21, no. 5, Article ID 053002, 2019.

[13] T. Banerjee and D. Ghosh, "Transition from amplitude to oscillation death under mean-field diffusive coupling," *Physical Review A*, vol. 89, no. 5, Article ID 052912, 2014.

[14] D. Ghosh and T. Banerjee, "Transitions among the diverse oscillation quenching states induced by the interplay of direct and indirect coupling," *Physical Review A*, vol. 90, no. 6, Article ID 062908, 2014.

[15] K. Sathiyadevi, D. Premraj, T. Banerjee, Z. Zheng, and M. Lakshmanan, "Aging transition under discrete time-dependent coupling: restoring rhythmicity from aging," *Chaos, Solitons & Fractals*, vol. 157, Article ID 111944, 2022.

[16] C. Xu, X. Tang, H. Lü et al., "Collective dynamics of heterogeneously and nonlinearly coupled phase oscillators," *Physical Review Research*, vol. 3, no. 4, Article ID 043004, 2021.

[17] X. Dai, X. Li, H. Guo et al., "Discontinuous transitions and rhythmic states in the D-dimensional Kuramoto model induced by a positive feedback with the global order parameter," *Physical Review Letters*, vol. 125, no. 19, Article ID 194101, 2020.

[18] A. A. Khatun, Y. A. Saeed, N. Punetha, and H. H. Jafri, "Collective dynamics of coupled Lorenz oscillators near the Hopf boundary: intermittency and chimera states," 2022, https://arxiv.org/abs/2207.09119.

[19] A. Koseska, E. Volkov, and J. Kurths, "Oscillation quenching mechanisms: amplitude vs. oscillation death," *Physics Reports*, vol. 531, no. 4, pp. 173–199, 2013.

[20] W. Zou, D. V. Senthilkumar, M. Zhan, and J. Kurths, "Quenching, aging, and reviving in coupled dynamical networks," *Physics Reports*, vol. 931, pp. 1–72, 2021.

[21] A. Koseska, E. Volkov, and J. Kurths, "Parameter mismatches and oscillation death in coupled oscillators," *Chaos: An Interdisciplinary Journal of Nonlinear Science*, vol. 20, no. 2, Article ID 023132, 2010.

[22] A. Zakharova, I. Schneider, Y. N. Kyrychko et al., "Time delay control of symmetry-breaking primary and secondary oscillation death," *EPL*, vol. 104, no. 5, Article ID 50004, 2013.

[23] K. Ponrasu, K. Sathiyadevi, V. K. Chandrasekar, and M. Lakshmanan, "Conjugate coupling-induced symmetry breaking and quenched oscillations," *EPL*, vol. 124, no. 2, Article ID 20007, 2018.

[24] K. Sathiyadevi, V. K. Chandrasekar, D. V. Senthilkumar, and M. Lakshmanan, "Distinct collective states due to trade-off between attractive and repulsive couplings," *Physical Review A*, vol. 97, no. 3, Article ID 032207, 2018.

[25] A. Zakharova, M. Kapeller, and E. Schöll, "Chimera death: symmetry breaking in dynamical networks," *Physical Review Letters*, vol. 112, no. 15, Article ID 154101, 2014.

[26] I. Gowthaman, K. Sathiyadevi, V. K. Chandrasekar, and D. V. Senthilkumar, "Symmetry breaking-induced state-dependent aging and chimera-like death state," *Nonlinear Dynamics*, vol. 101, no. 1, pp. 53–64, 2020.

[27] K. Sathiyadevi, S. Karthiga, V. K. Chandrasekar, D. V. Senthilkumar, and M. Lakshmanan, "Frustration induced transient chaos, fractal and riddled basins in coupled limit cycle oscillators," *Communications in Nonlinear Science and Numerical Simulation*, vol. 72, pp. 586–599, 2019.

[28] K. Sathiyadevi, V. K. Chandrasekar, and D. V. Senthilkumar, "Inhomogeneous to homogeneous dynamical states through symmetry breaking dynamics," *Nonlinear Dynamics*, vol. 98, no. 1, pp. 327–340, 2019.

[29] S. Majhi, S. N. Chowdhury, and D. Ghosh, "Perspective on attractive-repulsive interactions in dynamical networks: progress and future," *Europhysics Letters*, vol. 132, no. 2, Article ID 20001, 2020.

[30] Y. Jiang, J. Wu, H. Yang et al., "Chimera States mediated by nonlocally attractive-repulsive coupling in Fitz-Hugh–Nagumo neural networks," *Chinese Journal of Physics*, vol. 66, pp. 172–179, 2020.

[31] Y. Chen, J. Xiao, W. Liu, L. Li, and Y. Yang, "Dynamics of chaotic systems with attractive and repulsive couplings," *Physical Review E - Statistical Physics, Plasmas, Fluids, and Related Interdisciplinary Topics*, vol. 80, no. 4, Article ID 046206, 2009.

[32] A. Sharma, "Explosive synchronization through attractive-repulsive coupling," *Chaos, Solitons & Fractals*, vol. 145, Article ID 110815, 2021.

[33] S. Liu, Z. Sun, N. Zhao, and W. Xu, "Explosive transition in coupled oscillators through mixed attractive-repulsive interactions," *International Journal of Bifurcation and Chaos*, vol. 32, no. 02, Article ID 2250018, 2022.

[34] N. Zhao, Z. Sun, X. Song, and Y. Xiao, "Amplitude death in multiplex networks with competing attractive and repulsive interactions," *Physica A: Statistical Mechanics and its Applications*, vol. 608, 2022.

[35] I. A. Shepelev, S. S. Muni, and T. E. Vadivasova, "Spatio-temporal patterns in a 2D lattice with linear repulsive and nonlinear attractive coupling," *Chaos: An Interdisciplinary Journal of Nonlinear Science*, vol. 31, no. 4, Article ID 043136, 2021.

[36] K. Huper and J. Trumpf, "Mathematical system theory: festschrift in honor of uwe helmke on the occasion of his sixtieth birthday," *IFAC-PapersOnLine*, vol. 50, no. 1, pp. 2708–2713, 2013.

[37] H. Ahmed, R. Ushirobira, and D. Efimov, "Robust global synchronization of Brockett oscillators," *IEEE Transactions on Control of Network Systems*, vol. 6, no. 1, pp. 289–298, 2019.

[38] H. Ahmed, R. Ushirobira, D. Efimov, L. Fridman, and Y. Wang, "Oscillatory global output synchronization of nonidentical nonlinear systems," *IFAC-PapersOnLine*, vol. 50, 2017.

[39] H. Ahmed, R. Ushirobira, and D. Efimov, "On robust synchronization of nonlinear systems with application to grid integration of renewable energy sources," *Annual Reviews in Control*, vol. 52, pp. 213–221, 2021.

[40] H. Ahmed, R. Ushirobira, and D. Efimov, "Experimental study of the robust global synchronization of Brockett oscillators," *European Physical Journal: Special Topics*, vol. 226, no. 15, pp. 3199–3210, 2017.